atmosphere

MDPI

Article

Supplementary Material: Sensitivity of Spring Phenology Simulations to the Selection of Model Structure and Driving Meteorological Data

Réka Ágnes Dávid [1], Zoltán Barcza [1,2,3,*], Anikó Kern [4], Erzsébet Kristóf [2], Roland Hollós [1,2], Anna Kis [1,2], Martin Lukac [3,5] and Nándor Fodor [6]

[1] Department of Meteorology, Eötvös Loránd University, H-1117 Budapest, Pázmány P. st. 1/A, Hungary; davidreka@caesar.elte.hu (R.Á.D.); zoltan.barcza@ttk.elte.hu (Z.B.); hollorol@rolandhollos.xyz (R.H.); kisanna@nimbus.elte.hu (A.K.[1,2]);
[2] Excellence Center, Faculty of Science, Eötvös Loránd University, H-2462 Martonvásár, Brunszvik u. 2., Hungary; ekristof86@caesar.elte.hu (E.K.)
[3] Faculty of Forestry and Wood Sciences, Czech University of Life Sciences Prague, 165 21 Prague 6, Kamýcká 129, Czech Republic; m.lukac@reading.ac.uk (M.L.)
[4] Department of Geophysics and Space Sciences, Eötvös Loránd University, H-1117 Budapest, Pázmány P. st. 1/A, Hungary; anikoc@nimbus.elte.hu (A.K.[4])
[5] Centre for Agri-Environmental Research, School of Agriculture, Policy and Development, University of Reading, Reading, Berkshire, RG6 6AR, UK
[6] Agricultural Institute, Centre for Agricultural Research, H-2462 Martonvásár, Brunszvik u. 2., Hungary; fodor.nandor@atk.hu (N.F.)
* Correspondence: zoltan.barcza@ttk.elte.hu

Citation: Dávid, R.Á.; Barcza, Z.; Kern, A.; Kristóf, E.; Hollós, R.; Kis, A.; Lukac, M.; Fodor, N. Supplementary Material: Sensitivity of Spring Phenology Simulations to the Selection of Model Structure and Driving Meteorological Data. *Atmosphere* **2021**, *12*, 963. https://doi.org/10.3390/atmos12080963

Academic Editor: Ioannis Charalampopoulos

Received: date
Accepted: date
Published: 27 July 2021

Publisher's Note: MDPI stays neutral with regard to jurisdictional claims in published maps and institutional affiliations.

Copyright: © 2021 by the authors. Licensee MDPI, Basel, Switzerland. This article is an open access article distributed under the terms and conditions of the Creative Commons Attribution (CC BY) license (http://creativecommons.org/licenses/by/4.0/).

SOS climatology

Table S1 presents performance metrics for the modelled SOS climatology maps relative to the reference dataset.

Table S1. Performance metrics for the SOS climatology maps. RMSE and bias are expressed by DOY, while R^2 is unitless.

phenology model	**CWM**	**WM**	**GSIM**	**CWM**	**WM**	**GSIM**	**CWM**	**WM**	**GSIM**
driving meteorology	**CarpatClim**			**FORESEE**			**ERA5**		
overall RMSE	7.3	7.6	9.2	7.4	7.4	10.0	7.5	7.7	12.1
0–100m RMSE	7.2	7.4	7.8	7.3	7.2	8.3	7.2	7.2	10.4
100–200m RMSE	8.2	8.3	10.4	8.3	8.3	11.8	8.4	8.8	13.6
200–700m RMSE	4.7	6.0	7.7	4.8	4.5	7.3	4.6	4.6	10.3
overall bias	-0.5	0.1	-4.4	-1.0	-0.9	-6.0	-0.5	-0.5	-9.4
0–100m bias	1.8	1.5	-3.3	1.6	0.9	-3.3	1.5	0.6	-7.7
100–200m bias	-1.8	-1.6	-5.8	-2.4	-2.7	-8.0	-1.6	-1.8	-10.7
200–700m bias	-1.1	1.9	-2.6	-1.9	0.5	-5.4	-1.4	1.0	-8.8
overall R^2	0.07	0.07	0.05	0.07	0.09	0.01	0.05	0.05	0.05
0–100m R^2	0.01	0	0.01	0	0.01	0	0	0	0.02
100–200m R^2	0	0	0	0	0.02	0.01	0.05	0.02	0.01
200–700m R^2	0.14	0.17	0.08	0.18	0.23	0.18	0.19	0.23	0.14

Interannual variability

Table S2 presents performance metrics for the annual median SOS dates relative to the observation-based dataset.

Table S2. Performance metrics for the calculated annual median SOS dates relative to the observation-based results. RMSE and bias are expressed by DOY, while R^2 is unitless.

phenology model	**CWM**	**WM**	**GSIM**	**CWM**	**WM**	**GSIM**	**CWM**	**WM**	**GSIM**
driving meteorology	**CarpatClim**			**FORESEE**			**ERA5**		
overall RMSE	6.4	6.7	8.9	6.0	6.5	8.6	6.3	6.7	11.0
0–100m RMSE	8.2	7.3	9.2	8.1	7.3	9.0	8.1	7.6	10.0
100–200m RMSE	6.3	6.7	9.0	6.0	7.0	9.0	6.2	6.9	11.1
200–700m RMSE	5.7	7.5	8.3	5.9	7.8	8.7	5.7	7.3	10.2
overall bias	0.6	0	-2.4	0.1	-0.9	-3.3	0.3	-0.6	-7.8
0–100m bias	3.5	2.1	0.1	3.6	2.3	0.9	3.2	1.7	-5.1
100–200m bias	0.4	-0.2	-2.4	-0.4	-1.8	-4.7	0.2	-0.4	-7.5
200–700m bias	-0.7	2.0	-0.5	-1.2	0.7	-4.1	-0.5	1.9	-7.1
overall R^2	0.10	0.41	0.03	0.14	0.45	0.06	0.12	0.45	0.21
0–100m R^2	0.17	0.42	0.08	0.18	0.41	0.08	0.19	0.41	0.23
100–200m R^2	0.11	0.40	0.04	0.17	0.46	0.12	0.14	0.41	0.17
200–700m R^2	0.03	0.16	0.01	0.04	0.17	0.05	0.04	0.17	0.06

All performance metrics were calculated at the pixel level as well. Statistical indicators are presented in Table S3 focusing on the 5th and 95th percentile of the error metrics that were calculated from the individual, pixel based time series.

Here we discuss the error metrics in more details that supplements Section 3.3 of the paper.

Table S3. Additional statistical information about the interannual variability of SOS calculated at the individual pixel level. The 5th and 95th percentiles of the pixel level statistics are presented. RMSE and bias are expressed by DOY, while R^2 is unitless.

phenology model	**CWM**	**WM**	**GSIM**	**CWM**	**WM**	**GSIM**	**CWM**	**WM**	**GSIM**
driving meteorology	**CarpatClim**			**FORESEE**			**ERA5**		
RMSE 5th perc	6.54	7.87	8.86	6.48	7.80	8.65	6.59	7.64	9.60
RMSE 95th perc	18.72	18.74	20.44	18.55	18.84	20.95	18.74	19.02	23.20
bias 5th perc	-10.95	-11.43	-14.90	-11.02	-12.54	-16.57	-11.58	-12.45	-20.04
bias 95th perc	10.95	11.49	9.02	10.46	9.92	8.09	10.64	10.44	2.89
R^2 5th perc	0	0	0	0	0	0	0	0.01	0
R^2 95th perc	0.24	0.39	0.19	0.25	0.39	0.23	0.24	0.40	0.27

RMSE

Concerning elevation classes, RMSE is the lowest above 200 m with CWM and GSIM (except ERA5-GSIM) and in the case of WM between 100 and 200 m. According to Table S3, RMSE is similar for the CWM and WM (6.5–18.7 and 7.6–19 days, respectively), while it is higher for the GSIM (8.6–23.2 days) which is consistent with the overall results presented in Table S2. However, we can conclude that the pixel based RMSE performance needs to be improved.

Bias

If the driving meteorological dataset is FORESEE then the bias is negative (early simulated SOS) at 100–200 m for all models, and even above 200 m in the case of CWM and GSIM. Below 100 m overestimation occurs, except in case of the ERA5-driven GSIM, though it still has negative bias for every elevation classes. Pixel based bias ranges between -11.6 and +10.9 days, -12.5 and +11.5 days and -20 and +9 days for the CWM, WM and GSIM, respectively.

R^2

Overall R^2 is higher for the 0–100 m elevation class than above (the exception is the FORESEE-driven GSIM and WM, and ERA5-driven WM, here the highest value belongs to 100–200 m). The R^2 values of the WM are the largest regardless of the meteorological database used. The FORSEE-WM combination has the highest R^2 (45.4%) explained variance (ERA5-WM is the second with 44.8%). At the pixel level, R^2 values are small for the CWM and GSIM (ranging both between 0 and 0.24 or 0.27, respectively). For the WM R^2 is between 0 and 0.40 at the pixel level.

As the WM looks most suitable to quantify the IAV of the country-median and the pixel based SOS dates in terms of explained variance, further investigation is recommended. Figure S1 shows the relationship between the observed and the FORESEE-driven WM based annual SOS medians for the 1982–2010 time period. Error bars representing uncertainty are also plotted for the NDVI3g based estimates. The figure suggests the model performs better for later SOS dates (symbols are closer to the 1:1 line). There is one outlier in the plot that represents 1988. In that year the observed SOS was DOY 94, while the model predicted SOS in DOY 108. Without this data point R^2 increases to 0.58. It means that though NDVI3g has a unique length, longer datasets might be more suitable for the analysis.

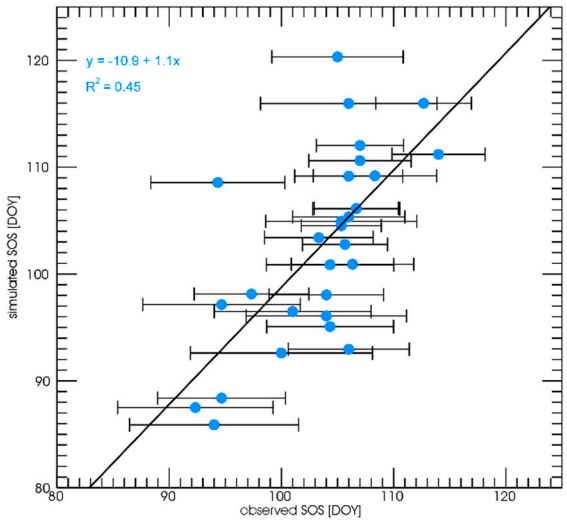

Figure S1. Relationship between the observation-based and the WM based annual median SOS dates for the 1982–2010 time period. Error bars represent +/- one standard deviation of the NDVI3g based SOS estimations. The equation of the fitted line is also presented (R^2 is significant with a *p*-value <0.0001).

Figure S2 shows the R^2 map for the WM driven by the FORESEE database (again, for 1982–2010). The map is in accordance with Table S2 in the sense that the model performs better below 200 m elevations (e.g. in the Great Plain of Hungary). The result is poor on the western border and in the north-east part of the country, and in some other locations as well. Land cover dependence was evaluated for the R^2 values. The analysis did not provide further insight into the behavior of the model, which means that spatially R^2 was not related e.g. to forest cover within the individual pixels.

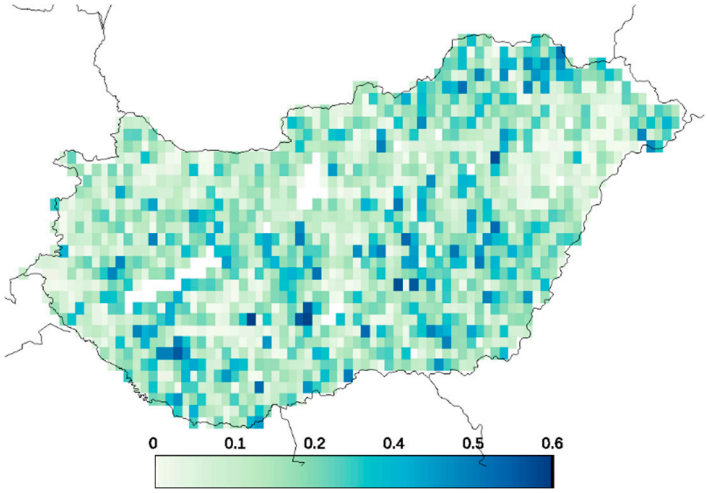

Figure S2. R^2 map based on the FORESEE-driven WM and the observations for the 1982–2010 time period.

Trend analysis

In order to provide more details about trend characteristics, pixel-based analysis was also performed. The results are presented in Figure S3 in the form of histograms. The figure shows that none of the model-database combinations is consistent with the observation-based estimates. It is clear that the frequency distributions are always narrower than the observation-based distribution. It means that the spatial variability of the decadal trend is not captured by the models. To illustrate the differences, if we select the FORESEE and CarpatClim database, the range of the trend values between the 5th and 95th percentiles are 2.4–2.9, 7.1–7.3, and 5.4–5.5 for the CWM, WM and GSIM, respectively, while it is 6.4 for the observations.

Figure S3 suggests that the CWM and the WM is relatively insensitive to the selection of the driving meteorological dataset, while GSIM results depend more on the driving meteorology. The distributions are typically shifted to the right (lower advancement) for the CWM, while they are shifted to the left with the WM. GSIM driven by ERA5 provides estimates that capture the middle of the histogram of the observations. This is the reason why the GSIM provided trend (for the entire target area) is consistent with the observation-based estimates.

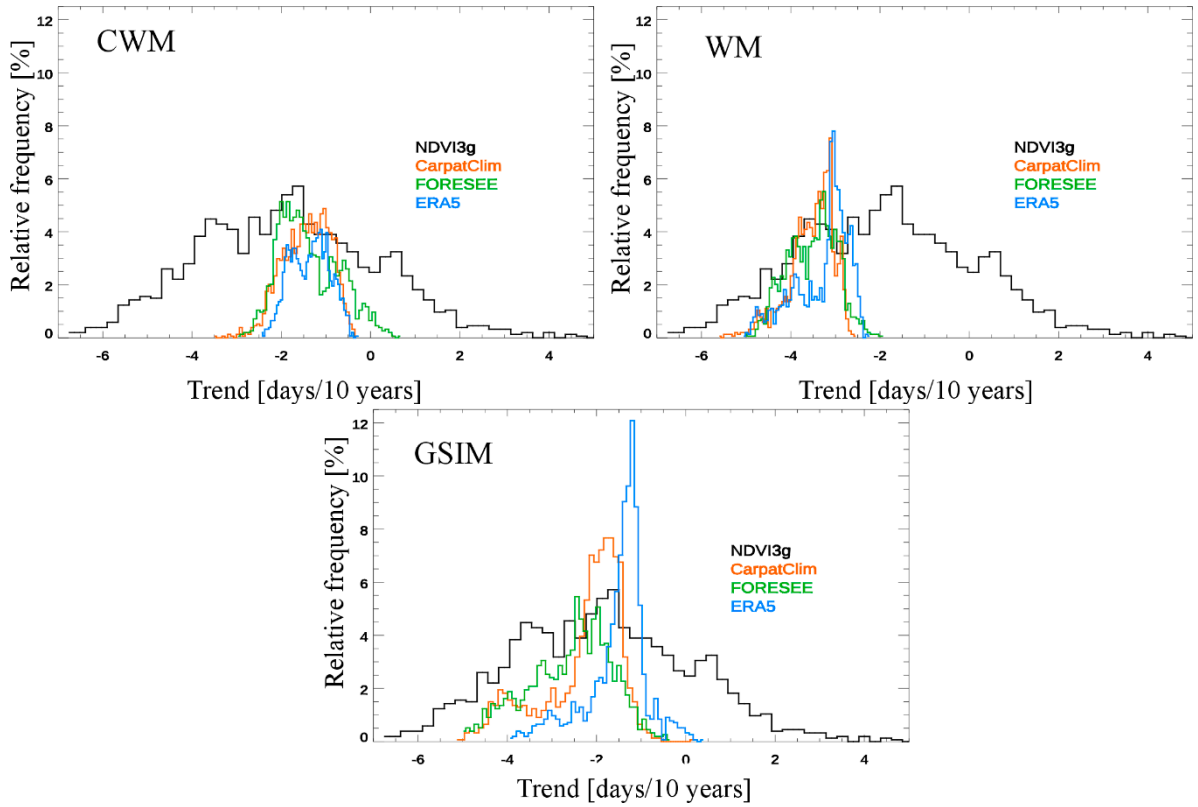

Figure S3. Frequency distribution of the pixel-based decadal trend values for the different models and the different driving datasets per model. The NDVI3g-based trend is presented in all plots to provide reference. The plot was constructed with data from all elevation classes together.